Size-controlled synthesis and characterization of thiol-stabilized gold nanoparticles

A. I. Frenkel,[a)] S. Nemzer, I. Pister, L. Soussan, and T. Harris
Physics Department, Stern College for Women, Yeshiva University, New York, New York 10016

Y. Sun and M. H. Rafailovich
Department of Materials Science and Engineering, State University of New York at Stony Brook, Stony Brook, New York 11733

Size-controlled synthesis of nanoparticles of less than a few nanometers in size is a challenge due to the spatial resolution limit of most scattering and imaging techniques used for their structural characterization. We present the self-consistent analysis of the extended x-ray absorption fine-structure (EXAFS) spectroscopy data of ligand-stabilized metal nanoclusters. Our method employs the coordination number truncation and the surface-tension models in order to measure the average diameter and analyze the structure of the nanoparticles. EXAFS analysis was performed on the two series of dodecanethiol-stabilized gold nanoparticles prepared by one-phase and two-phase syntheses where the only control parameter was the gold/thiol ratio ξ, varied between 6:1 and 1:6. The two-phase synthesis resulted in the smaller particles whose size decreased monotonically and stabilized at 16 Å when ξ was lowered below 1:1. This behavior is consistent with the theoretically predicted thermodynamic limit obtained previously in the framework of the spherical drop model of Au nanoparticles. © *2005 American Institute of Physics.* [DOI: 10.1063/1.2126666]

INTRODUCTION

The structure of ligand-stabilized gold clusters has been investigated experimentally[1–4] and theoretically[5–7] during the last decade. When the nanoclusters are smaller than 4–5 nm, i.e., the sizes typical for catalytic or biological applications, their three-dimensional structure can no longer be reliably determined by x-ray diffraction (XRD) because it drops below the minimum size of coherent scattering region that can be detected in XRD experiment. Other adequate techniques, e.g., electron microscopy, electron microdiffraction, or Mössbauer spectroscopy that can image even smaller particles are severely limited in characterizing nanoparticles *in situ*, i.e., simulating real reaction conditions that often require high temperatures, high pressures, and fast detection rates. Because of the lack of adequate experimental information, the large number of *ab initio* methods that propose different, often mutually exclusive stable structures of nanoparticles, cannot be directly verified. Under these limitations, the extended x-ray absorption fine-structure (EXAFS) technique emerges as the method of choice to analyze the nanoparticle structure, since it is suitable to address most problems that could not be tackled by other techniques *in situ*. Moreover, x-ray absorption spectroscopy is one of the premiere tools to study both atomic and electronic structures of small nanoparticle ensembles due, in part, to its local structure sensitivity and excellent spatial resolution. It can be done *in situ*, it is nondestructive to the nanoparticle, metal-support, and metal-ligand bondings, and it has become a common tool in studies of the nanoparticles and their applications in electrochemistry, electrocatalysis, and fuel cell developments.

In this work, we applied EXAFS to analyze the structure of thiol-protected gold nanoparticles that we synthesized by varying just one parameter: gold/thiol ratio (ξ). We discuss several strategies of EXAFS data modeling that use coordination number truncation and the surface tension in the framework of the spherical drop model. Our self-consistent modeling combines these techniques in order to obtain reliable information about the size and the structure of the nanoparticles at different values of ξ, from 6:1 to 1:6. The smallest of such particles (16 Å in diameter) were obtained by the two-phase synthesis at $\xi = 1:1$ and the average size did not change as the gold/thiol ratio was lowered to 1:6. We interpret this behavior in terms of surfactant-mediated stabilization of the particle size.[8]

SAMPLE PREPARATION AND EXPERIMENTS

The dodecanethiolate gold nanoparticles were synthesized using two methods: (1) a one-phase method developed by Yee *et al.*[9] and (2) a two-phase method developed by Brust *et al.*[10] The typical synthesis steps are described here for the both methods, using the Au/thiol ratio of 1:2 as an example.

In the one-phase method, 2.0 mmol of dodecanethiol was added under vigorous stirring to a solution of 1.1 mmol of hydrogen tetrachloroaureate (III) trihydrate $(\mathrm{H[Au(Cl_4)]} \cdot 3\mathrm{H_2O})$ in 30 mL of freshly distilled, anhydrous tetrahydrofuran (THF). The mixture was stirred for about 20 min at room temperature. 20 mL 1.0M solution of lithium triethylborohydride in THF was added slowly. The mixture turned dark purple immediately. After being stirred for 3 h,

---
[a)]Author to whom correspondence should be addressed. Electronic mail: anatoly.frenkel@yu.edu

TABLE I. Comparison of the bond contractions ΔR (in Å) obtained by EXAFS for the one-phase and two-phase synthesis methods.

Synthesis method	Au/thiol ratio (ξ)					
	1:6	1:3	1:2	1:1	3:1	6:1
One phase	⋯	0.022(3)	⋯	0.022(3)	0.022(3)	0.014(3)
Two phase	0.036(4)	0.035(4)	0.035(3)	0.034(3)	0.025(3)	0.018(3)

the mixture was mixed with 200 mL of absolute ethanol to precipitate the nanoparticles. The particles were centrifuged and washed with ethanol four times and dried in a vacuum desiccator.

In the two-phase method, an aqueous solution of $H[Au(Cl_4)] \cdot 3H_2O$ (1.1 mmol in 36 mL H_2O) was mixed with a solution of tetraoctylammonium bromide in toluene (4.8 mmol in 96 mL toluene). The two-phase mixture was vigorously stirred until all the tetrachloroaurate was transferred into the organic layer. 2.0 mmol dodecanethiol was then added. A freshly prepared aqueous solution of sodium borohydride (12 mmol in 30 mL water) was slowly added under vigorous stirring, the organic phase changed color from orange to deep brown within a few minutes. After being stirred for 3 h the organic phase was separated, evaporated to 5 mL in a rotary evaporator and mixed with 200 mL ethanol to remove excess thiol. The mixture was centrifuged to get the dark brown precipitate, which was washed with ethanol four times and dried in a vacuum desiccator.

Transmission electron microscopy (TEM) analysis was performed on a Philips CM12 STEM operating at 100 keV. The specimens were prepared by evaporating dilute solutions of nanoparticles in toluene onto the carbon-coated side of 400-mesh copper TEM grids. More than 500 particles were averaged to determine the average size of the nanoparticles for each value of ξ by the image contrast method. The results are summarized in Table I. Figure 1 shows several TEM micrographs and size distributions for particles prepared by the two-phase method at several values of ξ.

EXAFS experiments were performed at beamline X16C of the National Synchrotron Light Source, at Brookhaven National Laboratory. The specimens were prepared by spreading the powders onto adhesive tape and folding it up to 10–15 times until the desired thickness, corresponding to the Au L_3 absorption edge jump between 0.5 and 1.0, was achieved. X-ray absorption data from the sample and reference gold foil were measured in transmission mode at room temperature by scanning from 150 eV below to 1390 eV above the Au L_3 edge (11 917 eV). The reference Au foil was used to calibrate the x-ray energy during each scan and the data were aligned in absolute energy prior to the processing.

EXAFS DATA ANALYSIS

The analysis of EXAFS data was performed with the IFEFFIT package.[11] Figures 2 and 3(a) show the background-subtracted, edge step normalized, and k^2 weighted EXAFS data $\chi(k)$ in k space, and in r space, respectively. Fourier transforms were performed using a k range between 2 and 12 Å^{-1} and the Hanning window function with $\Delta k = 2$ Å^{-1}. The particles prepared by the two-phase method appeared smaller than those prepared by the one-phase method. Indeed, the particle size decrease lowers the amplitude of
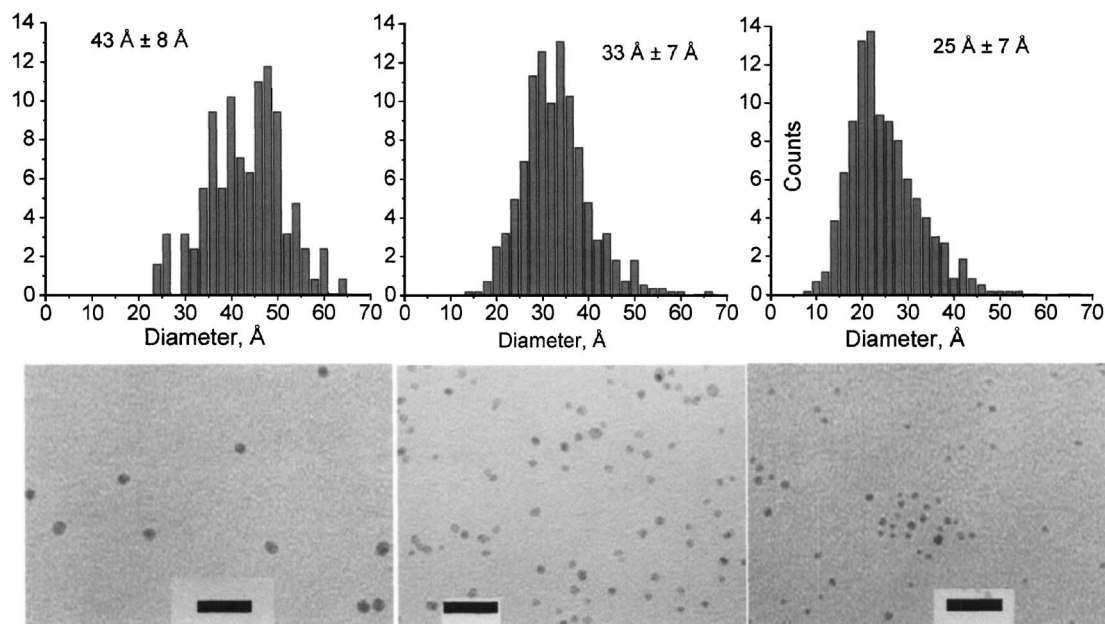
FIG. 1. Particle size dependence on Au/thiol ratio (ξ changes from 6:1 to 3:1 to 1:6 from left to right) as observed by TEM. The scale bar is 20 nm.
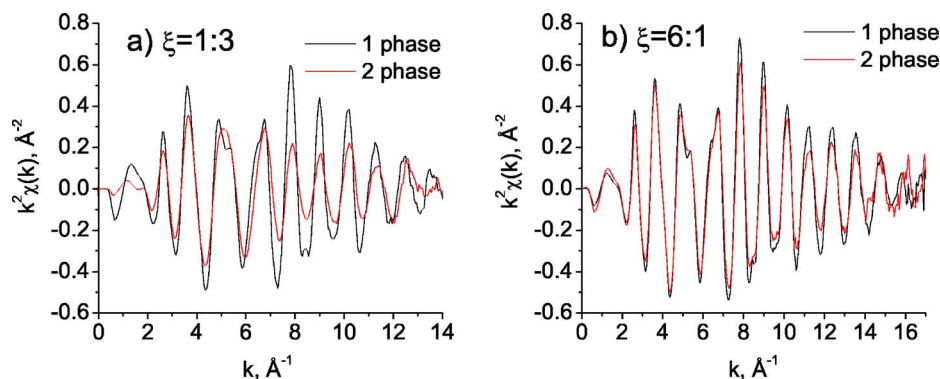
FIG. 2. (Color online) Difference in the average particle size between the samples synthesized by two different methods, as evident in their EXAFS data collected for the same values of ξ (1:3 and 1:6).

EXAFS oscillations due to the truncation effect [atoms on the surface of the particle are surrounded by fewer neighbors than those in the bulk and, hence, the average coordination number of the first nearest neighbors (1NN) decreases]. Figures 2(a) and 2(b) demonstrate that the EXAFS data measured in the samples prepared by the two different methods at the same ξ are different: the one-phase synthesis results in the larger amplitudes of EXAFS oscillations, due, apparently, to the larger average particle sizes.

It is also evident that the particle size reduces with lowering the Au/thiol ratio as inferred from the visible changes in the relative contributions of Au–Au and Au–S bonds to the Au L_3 EXAFS. The contributions of the Au–Au or Au–S interactions to EXAFS are progressively becoming less important, or more important, respectively, as ξ decreases [Fig. 3(a)].

Quantitative analysis was performed by fitting each data set with FEFF6 theory[12] in r space, using Au–S and Au–Au contributions to the theoretical EXAFS. The Au–Au FEFF theoretical photoelectron amplitudes and phases were calculated for the bulk Au structure. Its applicability to the nanoparticle structure that lacks long-range periodicity requires rigorous theoretical justification. However, the indirect evidence that the bulk photoelectron paths can be successfully used for the nanoparticle analysis stems from the good agreement between previous EXAFS and high-resolution TEM studies of the monodispersed Pt (Ref. 13) and Pt/Ru nanoparticles.[14] The variables in the fit were the coordination numbers of Au–S and Au–Au bonds, their distances and the disorders, σ^2 (or EXAFS Debye-Waller factors) in these distances. The passive electron reduction factor $S_0^2 = 0.825$ and the correction to the photoelectron energy origin were determined from the fits to the reference gold foil EXAFS and

fixed in the analysis of the nanoparticles. The total number of variables (6) was much smaller than the total number of the relevant independent data points (13).

The fit results were compared against the model containing an anharmonic correction (or third cumulant) to the theoretical EXAFS signal corresponding to the Au–Au pair. If anharmonicity is significant the average bond lengths would be larger than those when the anharmonicity is not accounted for. Thus, the role of the third cumulants in the fits is important to assess in order to avoid any ambiguity in the interpretation of the bond lengths obtained from the best fits. We obtained that including third cumulants in the theory did not affect the fit results outside of their uncertainties. Thus, the relative bond length changes (with respect to the bulk) that result from our modeling are not likely to be an artifact of the data analysis.

PARTICLE SIZE MODELING

Among EXAFS analysis results available for interpretation, we will examine most thoroughly the following two quantities: the coordination numbers N_{Au-Au} [Fig. 4(a)] of the 1NN Au–Au bonds, and the contractions of the 1NN bond lengths $\Delta R(\xi)$ [Table I, Fig. 4(b)]. The coordination numbers have been routinely used in previous EXAFS studies of nanoclusters in order to obtain their sizes, dating back to the earlier works[15,16] that used only the first shell analysis until the latest studies[13,17] where several NN shells, including multiple scatterings, were analyzed. The particle diameters can be estimated, among other methods, by assuming specific polyhedral shapes that Au nanoparticles can adopt: the icosahedral, cuboctahedral, and truncated octahedral are among the most commonly discussed geometries.[5,6]
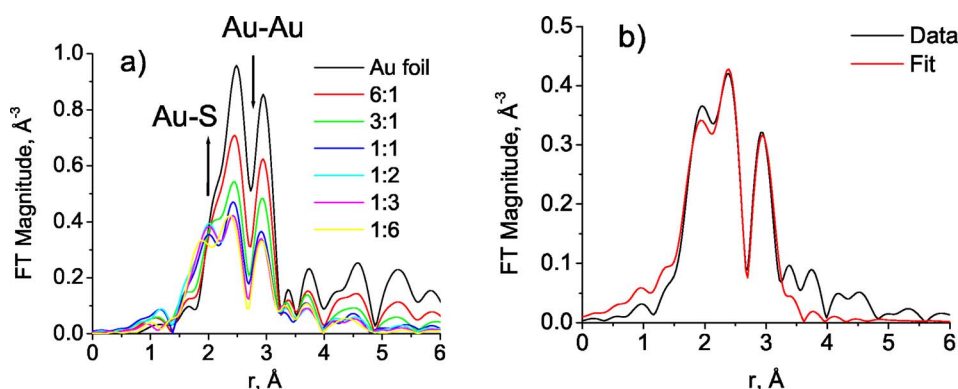
FIG. 3. (Color online) Particle size decrease and saturation is evidenced in EXAFS data of the samples prepared by the two-phase method. The relative numbers of Au–Au (Au–S) bonds decrease (increase) as ξ decreases (a). EXAFS data and theoretical fit (in r space) for the sample prepared by the two-phase method with ξ=1:3 (b).
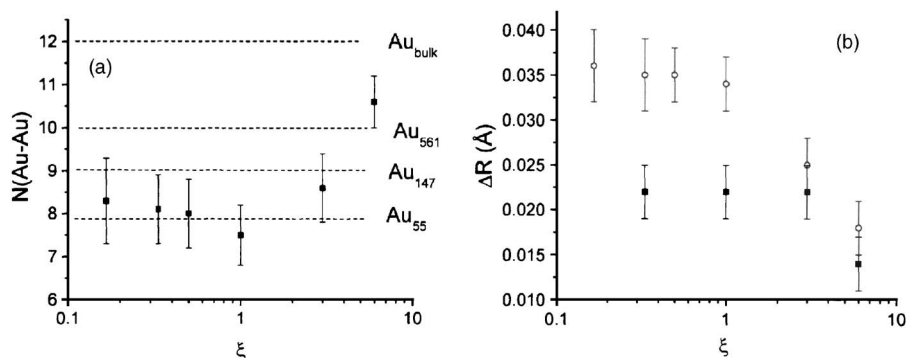
FIG. 4. (a) Size dependence of the average Au–Au coordination numbers for the samples prepared by the two-phase method. Shown by horizontal lines are the reference Au–Au coordination numbers in cubooctahedral clusters. (b) Size dependence of the average Au–Au 1NN distances (relative to the bulk) for the samples prepared by the one-phase method (filled squares) and the two-phase method (empty circles).

Based on the visual observation of the raw data [Fourier transform magnitudes in Fig. 3(a) have similar features in all samples, including Au foil, in the *r* range where Au–Au coordinations contribute], the icosahedral model was ruled out even in the smallest nanoparticles, and the cubooctahedral fcc structural model was assumed. In the icosahedral structure, the radial distribution of nearest neighbors is different from that in the fcc structure. Namely, the first shell, while being degenerate in the fcc structure, is split in the two subshells in the icosahedral structure due to 5% difference between the 1NN distances in the radial direction and within the icosahedral shell.[18] While insufficient spatial resolution may prevent direct observation of the splitting, the second nearest-neighbor shell, at distance $R_2 = \sqrt{2}R_1$, where R_1 is the 1NN distance, is clearly seen in fcc gold nanoparticles as the peak between 3.5 and 4 Å. Such group of distances, and the corresponding peak is absent in the icosahedral structure. This property has been recently utilized in the multiple-scattering analysis of monodisperse Au13 nanoclusters.[19]

In the present case, assuming the cubooctahedral fcc structure of all the particles, we calculated the number of atoms that idealized, monodispersed cubooctahedral nanoparticles would have in order to be characterized by the same Au–Au 1NN coordination numbers as those obtained in our EXAFS analysis. These "magic numbers" are indicated in Fig. 4(a) by horizontal lines. Using the ideal cubooctahedral models, we obtained the particle diameters from their Au–Au coordination numbers for different ξ (Fig. 5).

For all samples, the second quantity $\Delta R(\xi) = R_0 - R(\xi)$ where $R_0 = 2.88$ Å in bulk gold, and $R(\xi)$ is the bond length measured at the certain ξ, is obtained to decrease monotonically as ξ increases [Fig. 4(b)]. This effect of the 1NN distance shortening at smaller sizes should be attributed to the lattice contraction of closed-packed nanoparticles that has been previously interpreted in terms of surface stress. Following Mays *et al.*,[20] we relate the particle diameter *d* to the relative lattice contraction $\alpha = \Delta R / R$ via the surface stress f_{rr} and compressibility *K*,

$$d = \frac{4}{3} \frac{f_{rr} K}{\alpha}. \tag{1}$$

Using our EXAFS measurements of ΔR and *R* (Table I) as well as the experimentally determined values for *K* (5.99×10^{-13} cm^2/dyn),[20] f_{rr} (1175 dyn/cm) (Ref. 20) that were previously employed to obtain the size of the Au$_{55}$(PPh$_3$)$_{12}$Cl$_6$ nanoparticles,[21] we obtained the particle diameters for both the one-phase and two-phase preparation methods (Table II). The possibility that the surface stress and the compressibility may deviate in the nanoparticles from their bulk values is not accounted for in Eq. (1). However, following Woltersdorf *et al.*,[22] and Kern *et al.*,[23] we considered the size effect on f_{rr} and *K* to be insignificant. The fact that both (independent) techniques of EXAFS data analysis that we employed for the particle diameter determination (by using the coordination numbers and by using the distance contraction) obtain very similar results (Table II and Fig. 5) characterizes these results as highly reliable.

These figures demonstrate that the average sizes of the particles prepared by the two-phase method are smaller for the same value of ξ than those prepared by the one-phase method. This observation is supported by our TEM measurements for both types of particles. However, as Table II demonstrates, the average diameters obtained by TEM in both cases are consistently larger than the EXAFS-obtained diameters.
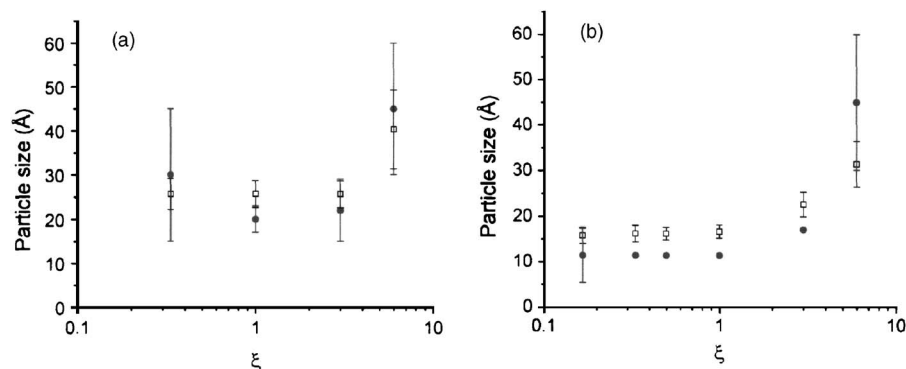
FIG. 5. Particle sizes for the samples prepared by the (a) one-phase and (b) two-phase methods. The sizes were obtained by EXAFS using two analysis techniques: empty squares indicate the surface tension technique [Eq. (1)], and filled circles were obtained from the coordination numbers characteristic for the cubooctahedral packing.

TABLE II. Comparison of the average particle sizes (in Å) obtained by EXAFS (using the coordination numbers truncation (CNT) and surface-tension (ST) techniques) and by TEM analyses. The numbers in parentheses are the uncertainties in the average size values (for the both EXAFS analysis techniques) and the standard deviation of the size distribution as obtained by TEM analysis.

Synthesis method	Analysis technique	Au/thiol ratio (ξ)					
		1:6	1:3	1:2	1:1	3:1	6:1
One-phase	$\langle d \rangle^{\mathrm{CNT}}_{\mathrm{EXAFS}}$	$\cdots$	30(15)	$\cdots$	20(3)	22(7)	45(15)
	$\langle d \rangle^{\Delta R}_{\mathrm{EXAFS}}$	$\cdots$	26(4)	$\cdots$	26(3)	26(3)	40(9)
	$\langle d \rangle_{\mathrm{TEM}}$	$\cdots$	42(10)	$\cdots$	36(10)	39(11)	30(10)
Two-phase	$\langle d \rangle^{\mathrm{CNT}}_{\mathrm{EXAFS}}$	11(6)	11.3	11.3	11.3	17.0	45(15)
	$\langle d \rangle^{\Delta R}_{\mathrm{EXAFS}}$	16(2)	16(2)	16(1)	17(1)	23(3)	31(5)
	$\langle d \rangle_{\mathrm{TEM}}$	25(8)	25(8)	$\cdots$	$\cdots$	33(7)	43(8)

DISCUSSION

As predicted by Leff *et al.*[8] in the framework of the statistical thermodynamic theory, the thiol-capped gold nanoparticles reach the minimum size for a certain Au/thiol ratio (ξ_0) beyond which, for $\xi < \xi_0$, the thiols are present in solution as monomers. This prediction was supported by the experimentally determined minimum of 14.7 ± 3.7 Å of the gold nanoparticle diameters using the Scherrer analysis of line broadening in x-ray powder-diffraction experiment.[8] Our results for the gold core sizes obtained by the new EXAFS analysis procedure (using the self-consistent measurements of Au–Au, Au–S coordination numbers, and Au–Au distance) for samples prepared by the two-phase synthesis are in good agreement with those obtained by Leff *et al.*[8] where the particles were synthesized by the same method. Namely, we also observed that the particle sizes decrease with the decrease of the Au/thiol ratio, and the gold core size stabilizes at its minimum value of 16 ± 2 Å, near the end of the $1:1 \leq \xi \leq 6:1$ composition range studied by Leff *et al.* In our work, we extended the composition range to $1:6 \leq \xi \leq 6:1$ that allowed us to investigate the saturation regime in greater detail. Using the extended range [Fig. 5(b)], we obtained the ratio at which the particle size stabilizes: $\xi_0 \approx 1:1$.

Based on the results of their EXAFS analysis of thiol-passivated gold nanoparticles, Zanchet *et al.*[24] argued that these nanoclusters' Au–Au distance contraction at small sizes should be weaker than that predicted by the simplified spherical drop model since the latter does not take into account strong gold-thiol interactions. Their results were later refined by Zhang and Sham,[25] who found that the lattice contractions for the same size Au nanoparticles as in Zanchet *et al.* were consistently stronger. We obtained relative contraction $\alpha = 1.3\%$ for our smallest (16 Å) nanoparticles, in excellent agreement with the result (1.4%) obtained by Zhang and Sham for the particles of the same size. However, Zanchet *et al.*, as well as Zhang and Sham, investigated only three different Au/thiol ratios: $\xi = 4:1$, 2:1 and 1:2,[24] and $\xi = 6:1$, 1:1 and 1:3.[25] Our analysis of six different samples is more systematic than those of Refs. 24 and 25. On one hand, we demonstrate similar distance contraction as in Zhang and Sham. On the other hand, we observe size saturation behavior, in excellent agreement with the more accurate model of nanoparticle energetics,[8] that takes into account gold-thiol,

thiol-thiol, and thiol-toluene interactions. Since our results for the nanoparticle diameters obtained by the spherical drop model [Eq. (1)] and the surface truncation model agree well for both one-phase and two-phase syntheses (Fig. 5), we conclude that the spherical drop model can be used to predict the Au–Au distance contraction even at relatively small particle sizes available in this experiment (ca. 16 Å).

Comparison of different methods of nanoparticle size determination, within the same technique (as in the present work) or between different methods[26] is required in order to obtain unambiguous results. In some cases, different methods complement each other, and their difference can be interpreted for positive sample characterization. For example, while the TEM results obtained in this work by the image contrast measurement overestimated the average particle size due to this method's relatively poor sensitivity to the small gold particles, smaller than ca. 2 nm (Table II), they provided information about the polydispersity of the particle sizes (Fig. 1), the information that XRD or EXAFS analyses are lacking.

Another technique commonly employed for the nanoparticle size determination is Scherrer analysis.[27] When the samples are polydispersed, the Scherrer analysis, which neglects effects of polydispersion, tends to overestimate the particle size as well.[26] On one hand, the EXAFS-based particle size determination method, particularly the one that uses coordination number truncation (CNT) analysis, may underestimate the average size for the polydispersed samples, especially if the radial distribution function is bimodal,[26] since the coordination numbers change nonlinearly with the particle size (Ref. 13). The surface-tension (ST) method, however, is more sensitive to the actual particle sizes than the CNT method because distance information is obtained in the form of both the mean bond length and, for quasi-Gaussian distributions, its standard deviation, or EXAFS Debye-Waller factor σ^2. For polydispersed particles, assuming a unimodal distribution that is consistent with our experimental data (Fig. 1), the majority of Au–Au 1NN bond lengths R may be placed within one standard deviation from the mean: $R_- < R < R_+$, where $R_- = R_0 - \sigma$, and $R_+ = R_0 + \sigma$. This range of distances corresponds, in turn, to the range of distance contraction factors, $\alpha_- < \alpha < \alpha_+$ and, eventually, to the range of the particle sizes $d_- < d < d_+$ that can be obtained experimen-

tally using Eq. (1). It is important to comment that the σ^2 used in this analysis is not the total Debye-Waller factor that includes both thermal (dynamic) and configurational (static) components, but just the static contribution to it, due to the polydispersity of the particle sizes, because Eq. (1) was obtained for thermally averaged 1NN distances in an ideal single particle.

Thermal disorder of the order of 0.008 Å^2 was obtained in the present work for the reference Au foil at room temperature. Thus, the difference between the experimentally measured σ^2 in the nanoparticles and the reference value of 0.008 Å^2 is the static contribution that contains information about the polydispersity of the particle sizes, because the dynamic contribution to the total Debye-Waller factor is relatively independent of the particle size.[13] In the present case, the static σ^2 was obtained to be equal to 0.003 Å^2. This value is too large, indicating that our size distribution is broad (in independent confirmation of Fig. 1 obtained by TEM), which prevents us to put reasonable brackets on the particle size range by the ST analysis method. This information can be extracted in principle for narrower distributions.

For the particles prepared by the one-phase synthesis, we obtained that the particle sizes were larger than their counterparts prepared by the two-phase synthesis. The origin of such difference is under investigation but our preliminary analysis by high-resolution electron microscopy measurements found evidence of multiple twinning in the gold core structure in the particles prepared by the one-phase synthesis.[28] Thus, the average ξ-d dependence for those particles cannot be described by the simplified spherical drop model.

SUMMARY AND CONCLUSIONS

We synthesized two different sets of thiol-stabilized gold nanoparticles (with Au/thiol ratios varying from 1:6 to 6:1 in each set) by the one-phase and two-phase synthetic routes. We analyzed the particle size distributions by a combination of two EXAFS analysis methods: the coordination number truncation method and the surface-tension method. These techniques were shown to be superior over the TEM that overestimates particle sizes at the small Au/thiol ratios. We obtained that the one-phase synthesis results in larger particles for the same Au/thiol ratio. For both synthetic routes, we obtained that the mean cluster size can increase/decrease as a result of changing a single parameter: the Au/thiol concentration. For the particles prepared by the two-phase route, we analyzed the data self-consistently, applying the coordination number truncation and the surface-tension methods of EXAFS data analysis, that allowed us to obtain reliable results for the particle sizes at all Au/thiol ratios. The smallest particles, ca. 16±2 Å in diameter, were obtained when the Au/thiol ratio decreased below 1:1. The particle size stabi-

lized at that value when Au/thiol ratio further decreased to 1:6, in agreement with the theoretically predicted thermodynamic limit obtained previously in the framework of the spherical drop model of Au nanoparticles.

[1] A. C. Templeton, W. P. Wuelfing, and R. W. Murray, Acc. Chem. Res. **33**, 27 (2000).
[2] S. Chen, A. C. Templeton, and R. W. Murray, Langmuir **16**, 3542 (2000).
[3] E. L. Whetten, J. T. Khoury, M. M. Alvarez, S. Murthy, I. Vezmar, Z. L. Wang, T. W. Stephens, C. L. Cleveland, W. D. Luedtke, and U. Landman, Adv. Mater. (Weinheim, Ger.) **5**, 428 (1996).
[4] P. M. Paulus, A. Goossens, R. C. Thiel, A. M. van der Kraan, G. Schmid, and L. J. de Jongh, Phys. Rev. B **64**, 205418 (2001).
[5] C. L. Cleveland, U. Landman, M. N. Shafigullin, P. W. Stephens, and R. L. Whetten, Z. Phys. D: At., Mol. Clusters **40**, 503 (1997).
[6] H. Häkkinen, R. N. Barnett, and U. Landman, Phys. Rev. Lett. **82**, 3264 (1999).
[7] C. L. Cleveland, U. Landman, T. G. Schaaff, M. N. Shafigullin, P. W. Stephens, and R. L. Whetten, Phys. Rev. Lett. **79**, 1873 (1997).
[8] D. V. Leff, P. C. Ohara, J. R. Heath, and W. M. Gelbart, J. Phys. Chem. **99**, 7036 (1995).
[9] C. K. Yee, R. Jordan, A. Ulman, H. White, A. King, M. Rafailovich, and J. Sokolov, Langmuir **15**, 3486 (1999).
[10] M. Brust, M. Walker, D. Bethell, D. J. Schiffrin, and R. J. Whyman, J. Chem. Soc., Chem. Commun. 1994, 801.
[11] M. Newville, J. Synchrotron Radiat. **8**, 322 (2001).
[12] S. I. Zabinsky, J. J. Rehr, A. Ankudinov, R. C. Albers, and M. J. Eller, Phys. Rev. B **52**, 2995 (1995).
[13] A. I. Frenkel, C. W. Hills, and R. G. Nuzzo, J. Phys. Chem. B **105**, 12689 (2003).
[14] M. S. Nashner, A. I. Frenkel, D. L. Adler, J. R. Shapley, and R. G. Nuzzo, J. Am. Chem. Soc. **119**, 7760 (1997).
[15] G. H. Via, J. H. Sinfelt, and F. W. Lytle, J. Chem. Phys. **71**, 690 (1979).
[16] R. B. Greegor and F. W. Lytle, J. Catal. **63**, 476 (1980).
[17] A. I. Frenkel, J. Synchrotron Radiat. **6**, 293 (1999).
[18] A. J. Mackay, Acta Crystallogr. **15**, 916 (1962).
[19] L. D. Menard, R. G. Nuzzo, A. I. Frenkel *et al.* (unpublished).
[20] C. W. Mays, J. S. Vermaak, and D. Kuhlmann-Wilsdorf, Surf. Sci. **12**, 134 (1968).
[21] M. C. Fairbanks, R. E. Beinfeld, R. J. Newport, and G. Schmid, Solid State Commun. **73**, 431 (1990).
[22] J. Woltersdorf, A. S. Nepijko, and E. Pippel, Surf. Sci. **106**, 64 (1981).
[23] R. Kern, G. Le Lay, and J. J. Metois, in *Current Topics in Materials Science*, edited by E. Kaldis (North-Holland, Amsterdam, 1979), Vol. 3, pp. 131–419.
[24] D. Zanchet, H. Tolentino, M. C. Martins Alves, O. L. Alves, and D. Ugarte, Chem. Phys. Lett. **323**, 167 (2000).
[25] P. Zhang and T. K. Sham, Phys. Rev. Lett. **90**, 245502 (2003).
[26] S. Calvin, M. M. Miller, R. Goswami, S.-F. Cheng, S. P. Mulvaney, L. J. Whitman, and V. G. Harris, J. Appl. Phys. **778**, 94 (2003).
[27] P. Zhang and T. K. Sham, Appl. Phys. Lett. **81**, 736 (2002).
[28] Y. Sun, A. I. Frenkel, N. Chi, N.-L. Yang, H. Xu, J. Yang, M. Rafailovich, and J. Sokolov (unpublished).